

## Aberystwyth University

### *Molecular organization in organic semiconductor thin films observed in real time*

Evans, D. A.; Roberts, O. R.; Vearey-Roberts, Alex Raymond; Williams, G. T.; Brieva, Abel; Langstaff, D. P.

*Published in:*  
Applied Physics Letters

*DOI:*  
[10.1063/1.4775762](https://doi.org/10.1063/1.4775762)

*Publication date:*  
2013

*Citation for published version (APA):*

Evans, D. A., Roberts, O. R., Vearey-Roberts, A. R., Williams, G. T., Brieva, A., & Langstaff, D. P. (2013). Molecular organization in organic semiconductor thin films observed in real time. *Applied Physics Letters*, 102(2), [021605]. <https://doi.org/10.1063/1.4775762>

#### **General rights**

Copyright and moral rights for the publications made accessible in the Aberystwyth Research Portal (the Institutional Repository) are retained by the authors and/or other copyright owners and it is a condition of accessing publications that users recognise and abide by the legal requirements associated with these rights.

- Users may download and print one copy of any publication from the Aberystwyth Research Portal for the purpose of private study or research.
- You may not further distribute the material or use it for any profit-making activity or commercial gain
- You may freely distribute the URL identifying the publication in the Aberystwyth Research Portal

#### **Take down policy**

If you believe that this document breaches copyright please contact us providing details, and we will remove access to the work immediately and investigate your claim.

tel: +44 1970 62 2400  
email: [is@aber.ac.uk](mailto:is@aber.ac.uk)

## Molecular organization in organic semiconductor thin films observed in real time

D. A. Evans, O. R. Roberts, A. R. Vearey-Roberts, G. T. Williams, A. C. Brieva et al.

Citation: *Appl. Phys. Lett.* **102**, 021605 (2013); doi: 10.1063/1.4775762

View online: <http://dx.doi.org/10.1063/1.4775762>

View Table of Contents: <http://apl.aip.org/resource/1/APPLAB/v102/i2>

Published by the [American Institute of Physics](#).

---

### Related Articles

An in situ x-ray photoelectron spectroscopy study of the initial stages of rf magnetron sputter deposition of indium tin oxide on p-type Si substrate

*Appl. Phys. Lett.* **102**, 021606 (2013)

Substrate orientation dependence on the solid phase epitaxial growth rate of Ge

*J. Appl. Phys.* **113**, 033505 (2013)

N incorporation in GaInNSb alloys and lattice matching to GaSb

*J. Appl. Phys.* **113**, 033502 (2013)

Thermal annealing effect on material characterizations of  $\beta$ -Ga<sub>2</sub>O<sub>3</sub> epilayer grown by metal organic chemical vapor deposition

*Appl. Phys. Lett.* **102**, 011119 (2013)

Crystallinity of inorganic films grown by atomic layer deposition: Overview and general trends

*J. Appl. Phys.* **113**, 021301 (2013)

---

### Additional information on *Appl. Phys. Lett.*

Journal Homepage: <http://apl.aip.org/>

Journal Information: [http://apl.aip.org/about/about\\_the\\_journal](http://apl.aip.org/about/about_the_journal)

Top downloads: [http://apl.aip.org/features/most\\_downloaded](http://apl.aip.org/features/most_downloaded)

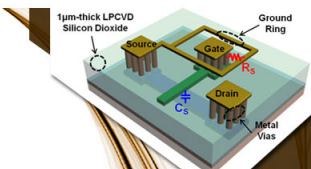
Information for Authors: <http://apl.aip.org/authors>

## ADVERTISEMENT

**AIP** | Applied Physics  
Letters


**EXPLORE WHAT'S  
NEW IN APL**

**SUBMIT YOUR PAPER NOW!**



**SURFACES AND  
INTERFACES**

Focusing on physical, chemical, biological, structural, optical, magnetic and electrical properties of surfaces and interfaces, and more...



**ENERGY CONVERSION  
AND STORAGE**

Focusing on all aspects of static and dynamic energy conversion, energy storage, photovoltaics, solar fuels, batteries, capacitors, thermoelectrics, and more...

# Molecular organization in organic semiconductor thin films observed in real time

D. A. Evans,<sup>a)</sup> O. R. Roberts, A. R. Vearey-Roberts, G. T. Williams,<sup>b)</sup> A. C. Brieva, and D. P. Langstaff

*Institute of Mathematics and Physics, Aberystwyth University, Aberystwyth SY23 3BZ, United Kingdom*

(Received 14 August 2012; accepted 27 December 2012; published online 17 January 2013)

Post-deposition molecular rearrangement in thin organic films is revealed by *in situ* real-time photoelectron spectroscopy during organic molecular beam deposition. Agreement between real time spectroscopy and Monte Carlo modeling confirms the role of nearest-neighbor molecular attraction in driving a time-dependent morphology for oriented films of tin phthalocyanine (SnPc) on a range of substrates. The time-dependent molecular self-organization occurs over timescales comparable to the growth rates and is therefore an important factor in the degradation of thin films of organic semiconductors typically considered for the fabrication of multilayer semiconductor devices. © 2013 American Institute of Physics. [<http://dx.doi.org/10.1063/1.4775762>]

Metal phthalocyanines are among the most robust, efficient, and cost-effective of organic semiconductors whose electronic, optoelectronic, and spin-conserving attributes offer applications such as photovoltaic cells,<sup>1</sup> Organic Light Emitting Diodes (OLED),<sup>2</sup> and organic spin valves.<sup>3</sup> The active organic layers are most commonly fabricated using vacuum sublimation, and it is usually assumed that the molecules rapidly organize into oriented films. However, using *in situ* electron spectroscopy applied in real time during organic molecular beam deposition, we have found that molecules of tin II phthalocyanine rearrange within grown films over remarkably long time scales that are greater than typical growth rates. This leads to significant time-dependent changes in the thin film morphology for a range of substrates. A mechanism is proposed for this process based on a slow molecular self-organization within the film that is confirmed using Monte-Carlo modeling.

Understanding the diffusion and self-organization of organic molecules in solids and liquids over appropriate energetic, temporal, and spatial ranges is crucial in understanding many natural and synthetic architectures. Ideally, experimental probes should be applied *in situ* and in real time to provide parallel and complementary information while being non-invasive in the formation process. This is rarely achievable, and most approaches involve one measurement technique probing one property. Examples include fluorescence microscopy for bio-molecule motion,<sup>4</sup> scanned-probe microscopy for nano-scale molecular motion,<sup>5</sup> and laser spectroscopy for ultrafast processes.<sup>6</sup> In each case, it is important to match the technique to the property under study.

In the fabrication of organic semiconductor devices, the probing method must be sensitive to molecular length scales in at least one dimension, it must resonate with the principal energy transfer mechanism in the solid and it must have the temporal resolution to probe either the individual molecular

motion or rate of processing. Such *in situ* techniques include x-ray diffraction,<sup>7</sup> electron diffraction,<sup>8</sup> and light scattering.<sup>9</sup> Photoelectron-based methods have the required inherent nano-scale sensitivity but are rarely used as a real-time probe since the data acquisition time is usually prohibitive.<sup>10–12</sup> Using a combination of a bright synchrotron light source and multichannel electron detection, coupled to theoretical modeling, we have been able to apply this method in real time to reveal the evolving organization of molecules during the growth of thin organic semiconductor films on different semiconductor and metal substrates.

Interfaces where small organic molecules such as SnPc are in contact with metals and other semiconductors are often the performance-limiting regions of electronic and photonic devices and the substrates in this study have been chosen in this context. Au is a common electrode and substrate for molecular adsorption; Si-organic systems are of broad interest in the integration of organic and inorganic technologies for example, for new bio-sensors and III-V-organic systems are of interest in photonic, electronic, and spintronic applications.<sup>13,14</sup>

Passivated H:Si(111) and S:GaAs(001) surfaces were initially prepared by chemical etching using HF (Ref. 15) and S<sub>2</sub>Cl<sub>2</sub> (Ref. 16), respectively, and polycrystalline gold substrates were polished and solvent cleaned. Following *in situ* annealing and (for Au) Ar ion sputtering, each substrate was in turn exposed to SnPc thermally evaporated from a shutter-controlled, water-cooled Knudsen cell with the molecular flux determined from a quartz crystal thickness monitor placed in the vicinity of the sample. The film thickness and morphology was confirmed using non-contact atomic force microscopy (AFM) in ambient conditions.

Fast photoelectron spectroscopy probing both core and occupied valence states has been enabled using a direct electron counting multi-channel array detector coupled to a conventional hemispherical array detector.<sup>12,17</sup> Tunable synchrotron radiation in the soft x-ray region enables valence and core level electron spectra to be recorded during growth using a single incident photon energy. All accessible substrate and overlayer core levels and band edges were monitored sequentially to provide a direct and parallel probe of the changing chemical,

<sup>a)</sup> Author to whom correspondence should be addressed. Electronic mail: [a.evans@aber.ac.uk](mailto:a.evans@aber.ac.uk).

<sup>b)</sup> Present address: Element Six Technologies Ltd., Ascot SL5 8BP, United Kingdom.

morphological, and electronic properties of the growing inorganic-organic interfaces. The experimental arrangement is illustrated schematically in Fig. 1(a). The focus here is on the evolving morphology of the organic film, hence consideration is given only to the variation in intensity of the principal core level emission peaks.

The Si 2p, As 3d, and Au 4f core level emission peaks for Si, GaAs, and Au substrates are shown in Fig. 1(b) along with snapshot spectra (open symbols) recorded in 700 ms, 250 ms, and 100 ms, respectively. The essential spectral features are reproduced by the rapidly collected snapshot spectra although there is some compromise in intensity and energy resolution. As an example of the time evolution of such photoelectron spectra, a sequence of Au 4f spectra recorded in real time during exposure of a polycrystalline gold substrate to a flux of SnPc is presented in Figure 1(c). Prior to exposure ( $t < 0$  s), there is no change in peak position or intensity. This confirms the stability of the measurement environment. During exposure ( $0 \text{ s} < t < 850 \text{ s}$ ), the doublet peak does not change in shape or position, but is significantly reduced in intensity. The constant line shape indicates a chemically undisrupted substrate. Similarly inert interfaces are found for Si and GaAs, and, for the Si(111) surface, the Si 2p core level peak is also unchanged in position during exposure to the SnPc molecules. The Fermi level position at the Si(111) surface is therefore unaffected by the organic adlayer. For the GaAs(001) surface, however, both As 3d and Ga 3d core levels in the GaAs move significantly during exposure indicating a strong organic-induced band-bending shift in the GaAs that is related to changes in interface state density and occupation.<sup>14</sup> When the SnPc cell shutter is closed at  $t = 850 \text{ s}$ , there is an increase in the Au 4f intensity and this unexpected effect is observed for all three substrates.

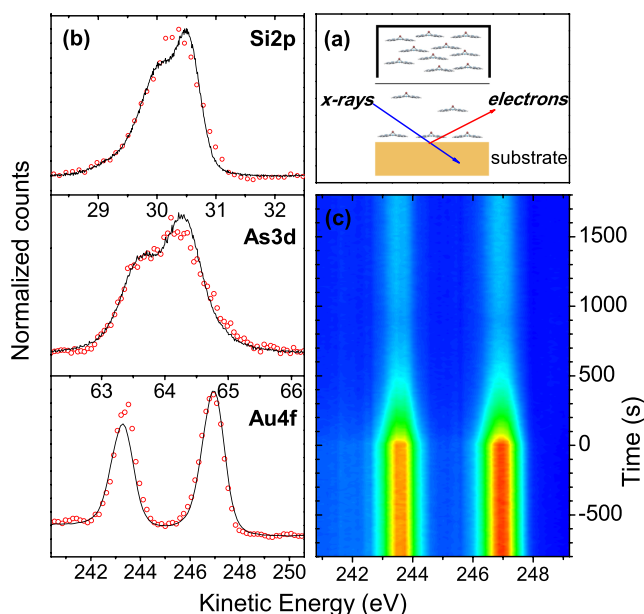


FIG. 1. (a) Schematic of the real-time monitoring of organic thin film growth. (b) Core level emission spectra for Si(111), GaAs(001) and polycrystalline Au. Snapshot spectra (open symbols) are shown superimposed on the scanned energy spectra (solid lines). As 3d spectra were recorded in 250 ms, Si 2p spectra were recorded in 750 ms and Au 4f spectra were recorded in 100 ms. (c) Time evolution of the Au 4f snapshot spectrum before, during and after exposure to the organic flux. The onset of exposure is shown as  $t = 0 \text{ s}$  and the exposure is turned off at  $t = 850 \text{ s}$ .

In each sequence of real-time core level spectra, a curve-fitting procedure was applied to extract the peak intensity and peak position for each core level. The time dependence of the peak intensity for each of the three substrate core levels is shown in Fig. 2. For all three, there is an initial rapid decrease in intensity is followed by a slower attenuation rate and surprisingly, when the SnPc flux is turned off, there is a recovery of the substrate peak intensity. These different regimes are defined by regions A-D as shown in Fig. 2. Region A corresponds to the steady-state prior to exposure of the substrate to the organic molecules where a constant intensity is measured. Regions B and C correspond to exposure of the substrates to SnPc. In Fig. 2, the time axis has been converted into SnPc coverage using deposition rates calibrated with reference to a quartz crystal thickness monitor. The closing of the shutter, indicated by the vertical line at  $t = 0 \text{ s}$ , marks the start of region D where, in each case, there is a slow recovery in the substrate peak intensity over many tens of minutes.

The initial rate of attenuation (region B) for each substrate can be modeled using a simple exponential expression for laminar growth. The fitted curves are shown as straight lines in the semi-logarithmic plots of Fig. 2. This model provides the mean free path of the photoelectrons at each kinetic energy, and these are presented in Table I. The values

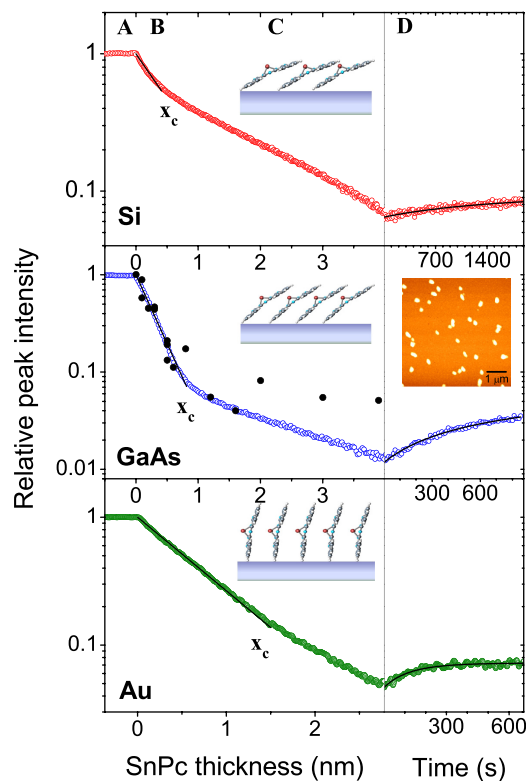


FIG. 2. Attenuation of the substrate core level peaks for SnPc adsorption on Si, GaAs and Au prior to SnPc exposure (region A), during exposure (regions B and C) and after exposure (region D). The molecular orientation within the first layer is illustrated for each substrate. The open symbols represent experimental points extracted from fitting sequences of Si 2p, As 3d, and Au 4f spectra and the large solid symbols for GaAs represent data acquired in conventional photoemission experiments. The solid lines are exponential fits to the real-time data in regions B and D. The final morphology, measured by ambient, non-contact AFM, for a 1 nm SnPc film is shown in the inset for GaAs.



TABLE I. Growth parameters for SnPc thin films on Si, GaAs, and Au substrates.

Substrate	Si	GaAs	Au
Mean free path/nm	0.6	0.3	0.8
Critical thickness/nm	0.4	0.9	1.5
Roughness/nm	0.1	1.0	30
Time constant/s	$1.8 \times 10^3$	$1.2 \times 10^3$	$1.4 \times 10^2$

range from 0.3 nm for the As 3d photoelectrons to 0.8 nm for the Au 4f photoelectrons and these map well to the universal curve that has a minimum for electron kinetic energies around 50 eV.<sup>18</sup> During exposure of each substrate to the molecular flux, there is a corresponding increase in the Sn 4d core level of the growing organic film<sup>19</sup> and this can also be modeled using a single exponential term with a similar electron escape depth. The growth of SnPc is thus uniform and 2-dimensional on each substrate up to a critical thickness,  $x_c$ , defined by the point of inflection separating regions B and C. The critical thickness can be accurately determined from the real-time data (Fig. 2) and a different value was obtained for each substrate as shown in Table I. This can be explained by considering the molecular structure within the organic films.

Planar molecules such as the metal phthalocyanines exhibit a range of substrate-dependent structural ordering with a general tendency to lay more parallel on a substrate when its surface is smooth.<sup>20</sup> The precise orientation of the SnPc molecules on flat substrates can be determined using angle-resolved x-ray absorption spectroscopy<sup>21</sup> and we have applied this technique to determine the orientation of SnPc molecules within our thin films. There is a well-defined orientation for SnPc molecules on both the Si(111) and GaAs(001) surfaces with calculated angles relative to the surface plane of 24° and 39°, respectively.<sup>19</sup> If it is assumed that the first layer is one molecule deep, then the thickness of this first layer is calculated to be 0.6 nm for Si and 0.9 nm for GaAs (based on a molecular diameter of 1.4 nm (Ref. 22)). These are close to the values of  $x_c$  determined from the data of Figure 2 (Table I), with a rather better agreement for the GaAs(001) substrate than the Si(111) substrate. No x-ray absorption measurements were possible for the gold substrate due to its roughness, but the value of  $x_c$  for this substrate is close to the diameter of the SnPc molecule and this would be consistent with a single molecular layer if the molecules were standing on end on this substrate. Interestingly, there appears to be a correlation between the molecular orientation and the surface roughness of each substrate as determined from non-contact AFM measurements (Table I), with the molecules standing up on the rough Au substrate while lying flatter on the smoother GaAs and Si substrates.

For thicknesses beyond  $x_c$  (region C), it is not possible to model the attenuation using a simple function, and this suggests a competition between at least two processes. Possible mechanisms for the observed reduction in the attenuation rate are enhanced inter-diffusion, increased desorption, and molecular clustering. Diffusion of molecules into the substrate is unlikely due to their size and this is supported by the absence of any spectral changes in the photoemission data

presented in Fig. 1. A second possibility is a reduction in the sticking coefficient for films of thickness greater than  $x_c$  due to desorption of molecules from the surface before becoming incorporated into the growing film. This has been reported for metal adsorption on III-V semiconductors at high temperatures.<sup>10</sup> For SnPc adsorption, desorption of the organic molecules is not likely to dominate at room temperature, although we have found that this effect becomes noticeable as the substrate temperature approaches the sublimation temperature at around 400 °C. The most likely mechanism is thus an enhanced clustering in the thicker films that results in 3-d island growth where molecules incident on the first wetting layer do not form uniform 2-d layers. The clustering model is preferred over the desorption model since *ex situ* AFM measurements (inset of Fig. 2) show that the total amount of SnPc is consistent with that predicted by photoemission assuming unity sticking coefficient. The AFM measurements also reveal an increased roughness of the deposited organic film in comparison with the clean substrate surfaces.<sup>23</sup> In region C, therefore, the molecules are more mobile than in region B with molecule-molecule interaction becoming significant. Further insights into this process are revealed in the data corresponding to region D, where the intensity profiles are recorded after closure of the SnPc evaporation cell. Surprisingly, a recovery in the substrate core level peak intensity (and a corresponding decrease in the organic core level peak intensity) was observed for each substrate.

It is possible to model this recovery process using an exponential function of the form  $I = I_0(1 - \exp[-\frac{t-t_0}{\tau}])$  to represent a time-dependent decrease in electron absorbing material and hence increase in the observed photoelectron intensity. For each substrate, the data could be modeled using a single time constant and this suggests that a simple, single process is responsible for the intensity recovery. This is in contrast, for example, to the desorption of Sb atoms from a heated GaSb surface where modeling of the data requires two time constants resulting from different adsorption sites.<sup>10</sup> The results of the fitting process for each of the three substrates are presented in Table I. The time constant is lowest for SnPc clustering on the roughest (Au) substrate where the molecules are standing up. For the smoother GaAs and Si surface, where the molecules are lying more parallel to the surface, the time constant for the intensity recovery is greater due to a lower molecular mobility. The time constant does however show some sensitivity to growth conditions such as the rate of arrival of the molecules and substrate temperature.

The time-dependent competition between adsorption and clustering is not usually observed in conventional photoemission measurements due to the long data acquisition times. This is illustrated in Fig. 2 for GaAs where real-time measurements (small open symbols) are compared with conventionally measured data (large solid symbols). During the initial uniform growth phase, the agreement is good but the data points diverge beyond the critical thickness. The conventional data in this region have higher intensities at the same nominal SnPc coverage, and this suggests that a more clustered film is formed in these slower experiments, where the SnPc film has time to relax between and during data acquisition. The data converge at longer times following recovery of the peak intensity in the real-time data.

AFM measurements confirm the clustered nature of the film as shown in the topography image in the inset of Fig. 2 for a SnPc film of nominal thickness 1 nm grown on GaAs and exposed to atmosphere. Cluster sizes of around  $20\text{ nm} \times 100\text{ nm}$  are observed and a similar cluster size has been reported for thicker films (10s–100s of nm) on this substrate.<sup>23</sup> It appears therefore that the clustering continues on exposure to air, with the molecules tending to cluster to a constant size. Rapidly grown films are uniform even at the lowest coverages, while thicker films that are allowed to relax are only fully uniform when the thickness is comparable to the cluster size ( $>20\text{ nm}$ ).

To account for the experimental data in region C, where the clustering process is competing with the adsorption of SnPc molecules, a more detailed model has been developed using a Monte-Carlo lattice-gas method.<sup>24,25</sup> In this model, the weakly interacting molecules are treated as flat-lying individual semi-transparent “tiles” which occupy points on a grid when deposited on a uniform surface.<sup>24</sup> They are allowed to re-organize but are not allowed to desorb from the surface. The substrate surface was modeled as a square-connected grid ( $N = 80 \times 80$ ) with periodic boundary conditions and orthogonal 4-fold connectivity and the transmission of radiation through the structure generated by the model was calculated by  $A = \frac{1}{N} \sum_{i=0}^N e^{-\lambda C_i}$  where  $\lambda$  is the extinction coefficient and  $C_i$  the total number of molecules at each point in the lattice.

Adsorption of molecules was simulated by placing  $n$  molecules per time step ( $n/N$  determines the deposition rate parameter) into random positions on the grid. At each timestep in the simulation, a Monte-Carlo component decides if the molecule at the top of each grid point is to be moved to a random neighboring site. The neighborhood surrounding each molecule is examined and a “binding” parameter,  $u$ , calculated, corresponding to the energy holding the molecule in place. The parameter,  $u$ , is calculated by  $u = g \times u_{\text{horizontal}} + u_{\text{vertical}}$ , where  $g$  is the number of adjacent cells containing equal or greater number of molecules,  $u_{\text{horizontal}}$  is the van der Waals force between adjacent molecules in the same plane, and  $u_{\text{vertical}}$  either the force between molecules in different planes or between a molecule and the substrate. The molecule is free to jump if  $e^{-\frac{u}{kT}} > p$ , where  $k$  is Boltzmann’s constant,  $T$  is the simulation temperature in K (normally 300 K), and  $p$  is a random number picked from a uniform distribution over the range 0 to 1. If the molecule is free to jump, then it is relocated to one of the orthogonally adjacent cells picked at random. During real deposition of material from a Knudsen cell, additional energy is supplied to the surface of the substrate by the impingement of the stream of supersonic particles, this is modeled in the simulation by allowing for a higher simulation temperature during the deposition phase (500 K).

In Fig. 3, an attenuation curve produced from the theoretical model by treating each molecule as a semi-transparent tile is presented (a) in comparison with experimental data for SnPc growth on polycrystalline gold (b). The simulated attenuation curve reproduces all the essential features of regions C and D in the experimental data, in particular the post-growth recovery in substrate intensity. The configurations of the molecules generated by the calculation at timesteps 5000 and 50000 are displayed as insets in Fig. 3 and these

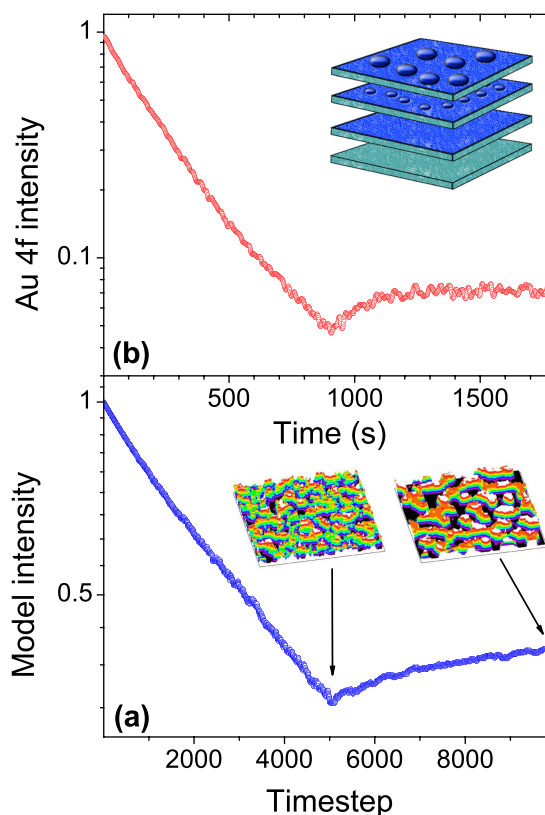


FIG. 3. (a) Monte Carlo modeling of the growth of an organic film to provide simulated total electron absorption through this film as a function of time. Also shown is the morphology of the film generated by the model at the end of exposure and following time-dependent molecular re-organization within the grown film. The model reproduces the experimentally observed attenuation and recovery of the transmitted electron intensity for SnPc adsorption and clustering on Au (b). The inset of (b) illustrates schematically the evolving morphology of the organic film.

reveal that the morphology of the film already shows signs of clustering at the end of the exposure in agreement with experiment. The islands become much more pronounced with time as the molecules organize slowly within the organic layer.

The experimentally observed photoelectron intensity variation is therefore determined by a competition between incorporation of molecules into the growing film and slow molecular re-organization within the film. Molecules in the first layer are locked in place by the dominant molecule-substrate attraction although the core level line shapes do not suggest strong charge transfer or covalent bond formation. Beyond the first layer, molecule-molecule attraction initiates cluster formation but this process is slow, with morphological changes occurring over the same timescale as thin film growth and the clustering continues for many tens of minutes after the organic flux has been removed. This has important consequences for multilayer thin film devices where the inter-molecular structure and film uniformity that determine the charge or spin transport can change significantly over long time scales. This slow self-organization also provides a way to engineer new blended structures using time as an additional control parameter in the fabrication process.

This work was supported by the EPSRC and the STFC and was performed within the Centre for Advanced Functional Materials and Devices, a HEFRCW Research and

Enterprise partnership. Dr. Jon Goss is thanked for calculated models of the SnPc molecular and electronic structure.

- <sup>1</sup>N. Li, B. E. Lassiter, R. R. Lunt, G. Wei, and S. R. Forrest, *Appl. Phys. Lett.* **94**, 023307 (2009).
- <sup>2</sup>S. R. Forrest, *Nature* **428**, 911 (2004).
- <sup>3</sup>V. Alek Dediu, L. E. Hueso, I. Bergenti, and C. Taliani, *Nat. Mater.* **8**, 707 (2009).
- <sup>4</sup>P. Kukura, H. Ewers, C. Muller, A. Renn, A. Helenius, and V. Sandoghdar, *Nat. Methods* **6**, 923 (2009).
- <sup>5</sup>E. Mateo-Marti, C. Rogero, C. Gonzalez, M. Sobrado, P. L. de Andres, and J. A. Martin-Gago, *Langmuir* **26**, 4113 (2010).
- <sup>6</sup>A. E. Ellen, H. G. Backus, A. W. Kleyn, and M. Bonn, *Science* **310**, 1790 (2005).
- <sup>7</sup>F. Schreiber, *Prog. Surf. Sci.* **65**, 151 (2000); S. Kowarik, A. Gerlach, and F. Schreiber, *J. Phys.: Condens. Matter* **20**, 184005 (2008).
- <sup>8</sup>R. R. Lunt, J. B. Benziger, S. R. Forrest, *Appl. Phys. Lett.* **90**, 181932 (2007).
- <sup>9</sup>D. E. Aspnes, J. P. Harbison, A. A. Studna, and L. T. Florez, *Phys. Rev. Lett.* **59**, 1687 (1987).
- <sup>10</sup>F. Maeda, Y. Watanabe, and M. Oshima, *Phys. Rev. Lett.* **78**, 4233 (1997).
- <sup>11</sup>F. Maeda and Y. Watanabe, *Appl. Surf. Sci.* **237**, 224 (2004); M. Rossi, B. S. Mun, Y. Enta, C. S. Fadley, K. Lee, S. Kim, H. Shin, Z. Hussain, and P. N. Ross, Jr., *J. Appl. Phys.* **103**, 044104 (2008).
- <sup>12</sup>D. A. Evans, O.R. Roberts, A. R. Vearey-Roberts, D. P. Langstaff, D. J. Twitchen, and M. Schwitters, *Appl. Phys. Lett.* **91**, 132114 (2007).
- <sup>13</sup>H. Ding, Y. Gao, M. Cinchetti, J.-P. Wustenberg, M. Sanchez-Albaneda, O. Andreyev, M. Bauer, and M. Aeschlimann, *Phys. Rev. B* **78**, 075311 (2008).
- <sup>14</sup>A. R. Vearey-Roberts and D. A. Evans, *Appl. Phys. Lett.* **86**, 072105 (2005).
- <sup>15</sup>S. Miyazaki, J. Schafer, J. Ristein, and L. Ley, *Appl. Phys. Lett.* **68**, 1247 (1996).
- <sup>16</sup>D. N. Gnoth, D. Wolframm, A. Patchett, S. Hohenecker, D. R. T. Zahn, A. Leslie, I. T. McGovern, and D. A. Evans, *Appl. Surf. Sci.* **123–124**, 120 (1998).
- <sup>17</sup>D. P. Langstaff, A. Bushell, T. Chase, and D. A. Evans, *Nucl. Instrum. Methods Phys. Res. B* **238**, 219 (2005).
- <sup>18</sup>M. P. Seah and W. A. Dench, *Surf. Interface Anal.* **1**, 2 (1979).
- <sup>19</sup>D. A. Evans, A. R. Vearey-Roberts, O. R. Roberts, A. C. Brieva, A. Bushell, G. T. Williams, D. P. Langstaff, G. Cabailh, and I. T. McGovern, *J. Vac. Sci. Technol. B* **28**, C5F5 (2010).
- <sup>20</sup>H. Peisert, T. Schwieger, J. M. Auerhammer, M. Knupfer, M. S. Golden, J. Fink, P. R. Bressler, and M. Mast, *J. Appl. Phys.* **90**, 466 (2001).
- <sup>21</sup>J. Stohr, *NEXAFS Spectroscopy* (Springer, Berlin, 1992), p. 403.
- <sup>22</sup>J. C. Buchholz and G. A. Somorjai, *J. Chem. Phys.* **66**, 573 (1977).
- <sup>23</sup>A. R. Vearey-Roberts, H. J. Steiner, S. Evans, I. Cerrillo, J. Mendez, G. Cabailh, S. O'Brien, J. W. Wells, I. T. McGovern, and D. A. Evans, *Appl. Surf. Sci.* **234**, 131 (2004).
- <sup>24</sup>I. Beichl and F. Sullivan, *IEEE Comput. Sci. Eng.* **4**, 91 (1997).
- <sup>25</sup>F. Elsholz, M. Meixner, and E. Scholl, *Nucl. Instrum. Methods Phys. Res. B* **202**, 249 (2003).